Cooperative Emission from an Ensemble of Three-Level Λ Radiators in a Cavity

Ryzhov, Igor V.; Vasil'ev, Nikolai N.; Kosova, Irina S.; Shtager, Maria D.; Malyshev, V.A.

Published in:
Journal of Experimental and Theoretical Physics

DOI:
10.1134/S1063776117050053

ISSN 1063-7761, Journal of Experimental and Theoretical Physics, 2017, Vol. 124, No. 5, pp. 683–700. © Pleiades Publishing, Inc., 2017.
Original Russian Text © I.V. Ryzhov, N.A. Vasil'ev, I.S. Kosova, M.D. Shtager, V.A. Malyshev, 2017, published in Zhurnal Eksperimental'noi i Teoreticheskoi Fiziki, 2017, Vol. 151, No. 5, pp. 803–822.

ATOMS, MOLECULES, OPTICS

Cooperative Emission from an Ensemble of Three-Level Λ Radiators in a Cavity: An Insight from the Viewpoint of Dynamics of Nonlinear Systems

I. V. Ryzhov[a]*, N. A. Vasil'ev[a], I. S. Kosova[a], M. D. Shtager[a], and V. A. Malyshev[b,c]

[a] *Herzen State Pedagogical University of Russia, St. Petersburg, 191186 Russia*
[b] *Fock Research Institute of Physics, St. Petersburg State University, St. Petersburg, 198504 Russia*
[c] *Zernike Institute for Advanced Materials, University of Groningen, AG Groningen, 9747 The Netherlands*
**e-mail: igoryzhov@yandex.ru*

Received September 14, 2015; in final form, September 15, 2016

Abstract—Cooperative radiation emitted by an ensemble of three-level optical systems with a doublet in the ground state (Λ scheme), which is placed into a cyclic cavity, is studied theoretically. In contrast to the two-level model of emitters, this process with such a configuration of operating transitions may occur without population inversion in the whole, if the doublet is prepared at the initial instant in a superposition (coherent) state. In the ideal case of a Hamilton system, in which the cavity losses and relaxation in the radiator ensemble are disregarded, the conservation laws are derived, which allow a substantial reduction of the dimension of the phase space of the model ($\mathbb{R}^{11} \to \mathbb{R}^5$) and the application of methods of dynamics of nonlinear systems for analyzing the three-level superradiance under these conditions. The possibility of different (both quasi-periodic and chaotic) scenarios of the three-level superradiance is demonstrated on the basis of Poincaré's mappings. Global bifurcation of the system upon a transition from the conventional superradiance regime to inversionless one is revealed. The effects of cavity losses, as well as homogeneous and inhomogeneous broadening in the system of radiators on the regularities found are also discussed.

DOI: 10.1134/S1063776117050053

1. INTRODUCTION

Sixty years ago, Dicke [1] predicted that a system of two-level atoms prepared at the initial instant in the excited state can emit collectively owing to correlation of emitters by the field of their own radiation. This phenomenon was later called coherent spontaneous emission (Dicke superradiance, SR). Dicke [1] considered a system with a linear size smaller than the radiation wavelength. In the 1970s (15 years after the SR prediction), Dicke investigations were further developed and generalized to extended systems in which SR exhibits peculiar properties [2–6]. Skribanowitz, Herman, MacGillivray, and Feld were the first to demonstrate in 1973 this effect experimentally on rotational transitions in the HF gas (see also [7–9]). Later, SR was observed in the solid phase [10–15], in spin systems [16–23], in generation of metastable states [24], in mesoscopic objects [25], in plasmon structures [26–28], and even in neutrino mass spectroscopy [29]. In should be noted in addition that Rayleigh scattering of light by a Bose–Einstein condensate of cold atoms is also of the SR origin [30–33], because the condensate preexists in the coherent state.

It is well known that the necessary condition for SR [1] to occur is the existence of initial population inversion of the transition levels [2–6, 34–39]. In the case of multilevel emitters (in particular, three level atoms with the Λ scheme of operating transitions considered here), this limitation is not necessary: SR is possible even when the initial population of the upper level is smaller than the population of the doublet (inversionless SR) [40–50]. A prototype of SR without the population inversion is the inversionless gain predicted for the first time in [51–53] (see also a review [54]). The essence of the effect can be described as follows. If the initial state of the lower doublet is prepared in the form of a coherent superposition, the transition to which from the upper state is forbidden, the orthogonal to it superposition, the transition to which is allowed, is found to be unpopulated in this case. Then the transition from the upper level to this superposition state turns out to be inverted for an arbitrarily small population of the upper level. This model was considered for

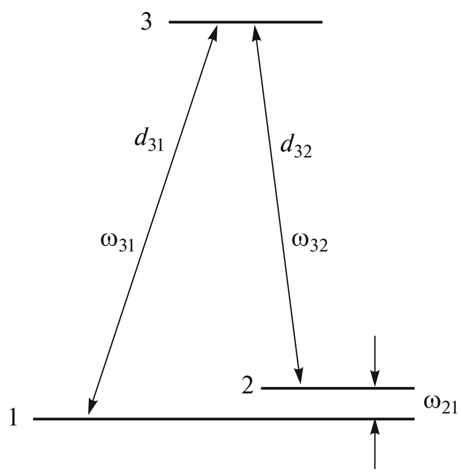

Fig. 1. Energy level diagram for a Λ emitter. Line number (n = 1, 2, 3) corresponds to the state of the emitter with energy E_n. Double arrows denote allowed transitions between the emitter levels, characterized by frequencies ω_{31} and ω_{32} and dipole moments d_{31} and d_{32} of the corresponding transitions; ω_{21} is the frequency of splitting of the doublet, the transition between the states of which is not considered.

the first time in [40–42] and later on (in greater detail) in [43], where it was found that the three-level SR exhibits various dynamic (even chaotic) regimes depending on the population of the upper level and doublet splitting. An attempt was made to interpret the detected regimes, but regular analysis has not been carried out.

The goal of the present work is to investigate theoretically the nonlinear dynamics of SR from an ensemble of three-level Λ atoms in a high-Q cyclic cavity, using consistently the dynamic theory of nonlinear systems (the model of the system and the formalism of its description are considered in Section 2). The main part of this research is devoted to the analysis of the conservative (Hamiltonian) model in which the relaxation of the population and electric polarization, associated with other (except SR) processes as well as the resonator losses are disregarded. The conservative nature of the system is manifested in the existence of integrals of motion, which (together with the special choice of initial conditions) make it possible to substantially reduce the dimension of the phase space of the model under investigation ($\mathbb{R}^{11} \to \mathbb{R}^5$, Section 3).

Our attention is mainly focused on analysis of the system with a nondegenerate doublet. The case with a degenerate doublet was investigated in detail in our previous publication [45]. We derive the equation for the SR field strength, which determines the stationary points of the system in the $\mathbb{R}^5$ phase space. The explicit form of this equation has made it possible to carry out the two-parametric (in parameters α and δ, where α is the initial population of the third level and δ is the doublet splitting) classification of these points and to determine range of their existence. It is shown that stationary points lie in the 3D subspace of the five-dimensional phase space, $\{A \in \mathbb{R}^3\} \subseteq \mathbb{R}^5$ (Section 4). The possibility of existence of quasi-periodic as well as chaotic regimes of three-level SR is demonstrated. In addition, the global bifurcation of the system upon a transition from the regime of conventional SR to the regime of SR without population inversion is revealed (Section 5). The mechanism driving the dynamic system to chaos and associated with a periodic approach of the system's phase trajectory to the separatrix where the conditions for a transition of the system to a qualitatively new phase trajectory occur, is considered in Section 6. Possible scenarios of system's randomization are also discussed. In the concluding part of this article (Section 7), we consider the effects of cavity losses as well as homogeneous and inhomogeneous broadening in the system of emitters on the possibility of realization of the regimes of three-level SR found and propose real-word systems in which such regimes can be observed.

2. MODEL AND FORMALISM

We consider an ensemble of three-level atoms with a Λ scheme of operating transitions (Fig. 1), which are distributed uniformly along one of the arms of a high-Q cyclic cavity. We disregard the effect of the active medium on the intrinsic cavity modes (i.e., we restrict our analysis to a so-called empty-cavity approximation). The search for modes of a cavity with an active medium is generally a complicated problem which is beyond the scope of this work. Optical transitions between upper state 3 and states 1 and 2 of the doublet are assumed to be allowed. The corresponding dipole moments $\mathbf{d}_{31}$ and $\mathbf{d}_{32}$ are likely being real-valued for simplicity. Optical transition frequencies ω_{31} and ω_{32} are considered to be distributed in a certain interval near their mean values $\bar{\omega}_{31}$ and $\bar{\omega}_{32}$ in accordance with the distribution functions $g_{31}(\omega)$ and $g_{32}(\omega)$ (inhomogeneous broadening). The transitions between the levels of the doublet are not considered, and doublet splitting frequency ω_{21} is assumed to be much smaller than frequencies ω_{31} and ω_{32}. For simplicity, we adopt that it is fixed and equal to $\bar{\omega}_{31} - \bar{\omega}_{32}$. This implies that frequencies $\bar{\omega}_{31}$ and $\bar{\omega}_{32}$ are shifted symbately (are correlated), and the distributions $g_{31}(\omega)$ and $g_{32}(\omega)$ are identical, but centered at frequencies $\bar{\omega}_{31}$ and $\bar{\omega}_{32}$, respectively. We do not consider the case of uncorrelated inhomogeneous broadening of the optical transition frequencies, which also leads to a inhomogeneous broadening of the doublet.

Optical dynamics of an isolated Λ atom is described by the density matrix ρ_{mn} (where m, n = 1, 2, 3), while the electric field strength $\mathbf{E}$ is governed by the Maxwell equation. In addition, all vectors (transition dipole moments and field polarization) are assumed to be codirectional and perpendicular to the axis of the system. Then the evolution of the atom + field system obeys the following (1D) system of the Maxwell–Bloch equations:

$$\dot{\rho}_{11} = \frac{1}{2T_1}\rho_{33} + i\frac{d_{31}E}{\hbar}(\rho_{31} - \rho_{13}),$$
$$\dot{\rho}_{22} = \frac{1}{2T_1}\rho_{33} + i\frac{d_{32}E}{\hbar}(\rho_{32} - \rho_{23}), \tag{1a}$$

$$\dot{\rho}_{33} = -\frac{1}{T_1}\rho_{33} - i\frac{d_{31}E}{\hbar}(\rho_{31} - \rho_{13}) - i\frac{d_{32}E}{\hbar}(\rho_{32} - \rho_{23}), \tag{1b}$$

$$\dot{\rho}_{21} = -i\omega_{21}\rho_{21} - i\frac{d_{31}E}{\hbar}\rho_{23} + i\frac{d_{32}E}{\hbar}\rho_{31}, \tag{1c}$$

$$\dot{\rho}_{31} = -\left(i\omega_{31} + \frac{1}{T_2}\right)\rho_{31} + i\frac{d_{31}E}{\hbar}(\rho_{33} - \rho_{11}) + i\frac{d_{32}E}{\hbar}\rho_{21}, \tag{1d}$$

$$\dot{\rho}_{32} = -\left(i\omega_{32} + \frac{1}{T_2}\right)\rho_{32} - i\frac{d_{32}E}{\hbar}(\rho_{33} - \rho_{22}) + i\frac{d_{31}E}{\hbar}\rho_{12}, \tag{1e}$$

$$\left(\frac{\partial^2}{\partial x^2} - \frac{1}{c^2}\frac{\partial^2}{\partial t^2}\right)E = \frac{4\pi}{c^2}\frac{\partial^2 P}{\partial t^2}. \tag{1f}$$

Here, T_1 and T_2 are the relaxation times for population and coherence, respectively; $1/T_2 = 1/(2T_1) + 1/T_2'$, T_2' being the coherence relaxation time that is not associated with the population relaxation; N is the concentration of active atoms in the substance; c is the speed of light in vacuum; and P is the polarization of the medium (dipole moment per unit volume), which is defined as

$$P = N\int d\omega[g_{31}(\omega)d_{31}\rho_{31} + g_{32}(\omega)d_{32}\rho_{32}] + \text{c.c.} \tag{2}$$

We have omitted for brevity the dependences of all functions in Eqs. (1) and (2) on coordinate, time, and frequency. The initial conditions for the density matrix elements and the field are given in the next section.

Let us further assume that frequencies ω_{31} and ω_{32} are quasi-resonant to one of cavity modes ω_c, and the SR spectrum does not exceed the gap between its modes; i.e., we restrict our analysis to the single-mode approximation. For simplifying the problem still further, we disregard the dependence of all dynamic variables on the spatial coordinate (mean field approximation). This approximation can be justified provided that a wave propagating in one direction is excited, and the time of the round trip of light over the cavity is much shorter than the SR characteristic time [43]. We will seek the solution to system of equations (1) in the form

$$\rho_{31} = \mathcal{R}_{31}e^{-i\omega_c t}, \quad \rho_{32} = \mathcal{R}_{32}e^{-i\omega_c t},$$
$$E = \mathcal{F}e^{-i\omega_c t} + \text{c.c.}, \tag{3}$$

where the amplitudes of the field $\mathcal{F}$ and off-diagonal elements $\mathcal{R}_{31}$ and $\mathcal{R}_{32}$ of the density matrix (henceforth referred to as high-frequency coherences) are the functions slowly varying on the scale of the optical period $2\pi/\omega_c$ (rotating wave approximation). It should be noted that no analogous assumption concerning low-frequency coherence ρ_{21} (on scale of $2\pi/\omega_{21}$) is used. For definiteness, we assume that the eigenfrequency ω_c of the cavity is centered between frequencies $\bar{\omega}_{31}$ and $\bar{\omega}_{32}$ (i.e., $\omega_c = (\bar{\omega}_{31} + \bar{\omega}_{32})/2$).

We also assume that the dipole moments of optical transitions are identical, $d_{31} = d_{32} = d$ (this approximation is not of principal importance). Note that the given problem is characterized by a quantity $\Omega = \sqrt{2\pi\omega_c d^2 N/\hbar}$, which is known in the literature as the cooperative frequency [38, 55] and determines the natural scales of time and field. Its physical meaning is that it is the Rabi frequency of the field with a number of photons equal to the number of atoms in the system [55]. Introducing dimensionless time $\tau = \Omega t$, relaxation constants $\tau_i = \Omega T_i$ ($i = 1, 2$), and the field amplitude $\mathcal{E} = -id\mathcal{F}/(\hbar\Omega)$ and passing in the standard manner from Eqs. (1) to an analogous system for the slowly varying amplitudes, we obtain

$$\dot{\rho}_{11} = \frac{1}{2\tau_1}\rho_{33} + \mathcal{E}\mathcal{R}_{31}^* + \mathcal{E}^*\mathcal{R}_{31},$$
$$\dot{\rho}_{22} = \frac{1}{2\tau_1}\rho_{33} + \mathcal{E}\mathcal{R}_{32}^* + \mathcal{E}^*\mathcal{R}_{32}, \tag{4a}$$

$$\dot{\rho}_{33} = -\frac{1}{\tau_1}\rho_{33} + \mathcal{E}(\mathcal{R}_{31}^* + \mathcal{R}_{32}^*) - \mathcal{E}^*(\mathcal{R}_{31} + \mathcal{R}_{32}), \tag{4b}$$

$$\dot{\rho}_{21} = -i\delta\rho_{21} + \mathcal{E}\mathcal{R}_{32}^* + \mathcal{E}^*\mathcal{R}_{31}, \tag{4c}$$

$$\dot{\mathcal{R}}_{31} = -\left[i\left(\Delta + \frac{\delta}{2}\right) + \frac{1}{\tau_2}\right]\mathcal{R}_{31} + \mathcal{E}(\rho_{33} - \rho_{22} - \rho_{21}), \tag{4d}$$

$$\dot{\mathcal{R}}_{32} = -\left[i\left(\Delta - \frac{\delta}{2}\right) + \frac{1}{\tau_2}\right]\mathcal{R}_{32} + \mathcal{E}(\rho_{33} - \rho_{22} - \rho_{21}^*), \tag{4e}$$

$$\dot{\mathcal{E}} = -\frac{1}{\tau_{\text{res}}}\mathcal{E} + \int d\Delta\left[g_{31}\left(\Delta - \frac{\delta}{2}\right)\mathcal{R}_{31} + g_{32}\left(\Delta + \frac{\delta}{2}\right)\mathcal{R}_{32}\right]. \tag{4f}$$

Here, $\Delta = (\omega_{31} - \bar{\omega}_{31})/\Omega = (\omega_{32} - \bar{\omega}_{32})/\Omega$ is the dimensionless detuning of optical transition frequencies from their mean values, $\delta = \omega_{21}/\Omega$ is the dimensionless frequency of doublet splitting, and $\tau_{\text{res}} = \Omega T_{\text{res}}$

is the dimensionless lifetime of the field in the cavity. This constant effectively takes into account the cavity losses in the mean field approximation [56].

3. HAMILTONIAN SYSTEM

Let us first consider in detail an ideal Hamiltonian system without relaxation in the system of emitters and with zero cavity losses: $T_1 = T_2 = T_{\text{res}} = \infty$, $g_{13}(\omega) = \delta(\omega - \bar{\omega}_{31})$, and $g_{32}(\omega) = \delta(\omega - \bar{\omega}_{32})$. The effect of these factors will be considered in the end of the article. In this case, the system of equations (4) has the following integrals of motion:

$$\rho_{11} + \rho_{22} + \rho_{33} = 1, \quad (5a)$$

$$\rho_{11}^2 + \rho_{22}^2 + \rho_{33}^2 + 2(|\rho_{21}|^2 + |\mathcal{R}_{31}|^2 + |\mathcal{R}_{32}|^2) = \text{const}, \quad (5b)$$

$$|\mathcal{E}|^2 + \rho_{33} = \text{const}, \quad (5c)$$

the first of which expresses the conservation law of the normalization and also holds in the general case in the presence of relaxation (homogeneous and inhomogeneous broadenings) and cavity losses. The second expression is just the conservation law for the trace of the density matrix squared. The interpretation of the last expression (5c) is not so obvious, although it resembles the conservation law for the excitation energy of the system. The existence of these integrals of motion makes it possible to substantially simplify analysis of the dynamics of three-level SR.

It should be emphasized that the Hamiltonian limit is fundamental and makes it possible to analyze stationary states of the system (see Section 4); it would hardly be possible to explain the optical dynamics of the system in the presence of relaxation (incoherent perturbations) without analyzing this limit. The allowance for any relaxation leads to violation of one of conservation laws (5) (see Section 7), thus increasing the dimension of the phase space and extremely complicating such analysis or even making it impossible. In such a case, the system of equations (4) has to be integrated numerically taking the relaxation into account, and its solution must be compared with the ideal (Hamiltonian) case (this will be done in Section 7). In this way, certain conclusions can be drawn concerning the optical dynamics of the system with relaxation and the time intervals, on which the Hamiltonian limit is observed, can be indicated.

As compared with two-level SR [37, 38], the scheme with a doublet in the ground state (three-level SR) introduces new effects in the response of the system, which are generated by the competition of transitions $|3\rangle \leftrightarrow |1\rangle$ and $|3\rangle \leftrightarrow |2\rangle$. For this reason, we choose the initial conditions for investigating the nonlinear dynamics of three-level SR in such a way that the interaction in the atoms + field system occurs most effectively (namely, for any initial population of the upper state and with the minimal delay of the SR pulse). In this connection, we note that Eqs. (4d) and (4e) for the high-frequency coherences ($\mathcal{R}_{31}$ and $\mathcal{R}_{32}$) contain the terms proportional to the low-frequency coherence ρ_{21}. Herewith, if $\rho_{21}(0) \neq 0$, the evolution of initial fluctuations $\mathcal{R}_{31}$ and $\mathcal{R}_{32}$ (decrease or increase) depends on the phase of $\rho_{21}(0)$. For positive values of $\rho_{21}(0)$, these fluctuations decrease, while for negative values, the fluctuations grow in an avalanche manner, thus initiating SR. From the standpoint of macroscopic electrodynamics, this indicates dissipative instability of the system [36]. It should be emphasized that this becomes possible for any difference of populations in the $3 \leftrightarrow 1$ and $3 \leftrightarrow 2$ channels and is ensured by the transformation of the low-frequency coherence $\rho_{21}(0)$ into the high-frequency coherences $\mathcal{R}_{31}$ and $\mathcal{R}_{32}$. The latter fact is reflected explicitly in the integral of motion (5b).

The pattern of formation of the SR dynamics of the given Λ system appears as especially clear in the new (collective) basis of states $|3\rangle$, $|+\rangle = (|1\rangle + |2\rangle)/\sqrt{2}$, $|-\rangle = (|1\rangle - |2\rangle)/\sqrt{2}$ [41, 43, 46, 48]. The transformation of the density matrix elements from the old basis to the new one is performed by the following relations:

$$\rho_{++} = \frac{1}{2}(\rho_{11} + \rho_{22} + 2\,\text{Re}[\rho_{21}]), \quad (6a)$$

$$\rho_{--} = \frac{1}{2}(\rho_{11} + \rho_{22} - 2\,\text{Re}[\rho_{21}]), \quad (6b)$$

$$\rho_{+-} = \frac{1}{2}(\rho_{11} - \rho_{22} + \rho_{21} - \rho_{21}^*), \quad (6c)$$

$$\mathcal{R}_{3+} = \frac{1}{\sqrt{2}}(\mathcal{R}_{31} + \mathcal{R}_{32}), \quad (6d)$$

$$\mathcal{R}_{3-} = \frac{1}{\sqrt{2}}(\mathcal{R}_{31} - \mathcal{R}_{32}), \quad (6e)$$

where ρ_{++} and ρ_{--} are the populations of the optically active (bright) and passive (dark) states; respectively; ρ_{+-} is the low-frequency coherence; and $\mathcal{R}_{3+}$ and $\mathcal{R}_{3-}$ are the high-frequency coherences of the corresponding optical channels.

The relation (6a) for the population of the bright state ρ_{++} shows that the condition for the existence of inversionless three-level SR is the presence of inversion in the active channel $|3\rangle \leftrightarrow |+\rangle$; i.e., an inequality $\rho_{33}(0) > \rho_{++}(0)$ must be satisfied at the initial instant. In the ideal case when the population of the bright state is zero,

$$\rho_{++}(0) = \rho_{11}(0) + \rho_{22}(0) + 2\,\text{Re}[\rho_{21}(0)] = 0,$$

the following conditions must be met:

$$\begin{gathered} \text{Re}[\rho_{21}(0)] = \frac{\alpha - 1}{2}, \quad \text{Im}[\rho_{21}(0)] = 0, \\ -2\,\text{Re}[\rho_{21}(0)] = \rho_{11}(0) = \rho_{22}(0), \end{gathered} \quad (7)$$

where $\rho_{33}(0) = \alpha$ and $0 < \alpha \leq 1$ as before. We will henceforth say that the doublet is prepared in the maximally coherent state if the conditions (7) are satisfied at the initial instant. It should be emphasized once again that for the given initial conditions, SR is possible for any initial population $\rho_{33}(0)$ of the upper state, even without inversion in the whole, when the total initial population of the doublet exceeds the initial population of the upper level ($\rho_{11}(0) + \rho_{22}(0) > \rho_{33}(0)$).

In the quantum-electrodynamic formulation of SR as a spontaneous process, the field and mean dipole moments are absent. Emission from the system is initiated by quantum fluctuations of the uncorrelated dipole moments of emitters. Phasing of the emitters occurs in the course of radiation. The semiclassical analog of this initial state consists in setting small random values of the amplitudes of high-frequency coherences $\mathcal{R}_{31}(0)$ and $\mathcal{R}_{32}(0)$ with certain correlation properties [57]. Another variant of the SR initiation involves applying a short (on the SR scale) small-area pulse that produces the deterministic and identical values of the amplitudes of high-frequency coherences $\mathcal{R}_{31}(0)$ and $\mathcal{R}_{32}(0)$ at each emitter, which exceed their quantum fluctuations (so-called triggered or induced SR [58, 59]). We will henceforth consider the second scheme of SR excitation. Thus, the initial conditions in the problem under investigation have the following form: the electric field strength is zero,

$$\mathrm{Re}[\mathscr{E}(0)] = \mathrm{Im}[\mathscr{E}(0)] = 0, \tag{8}$$

and a small uniform value of high-frequency coherences is set,

$$\mathrm{Re}[\mathcal{R}_{31}(0)] = \mathrm{Re}[\mathcal{R}_{32}(0)] = \pm R_0, \quad R_0 \ll 1, \tag{9}$$

where we assume without loss of generality that $\mathrm{Im}[\mathcal{R}_{31}(0)] = \mathrm{Im}[\mathcal{R}_{32}(0)] = 0$.

We have integrated numerically the system of differential equations (4) with the initial conditions (7)–(9) by varying two control parameter, viz., the initial population $\rho_{33}(0) = \alpha$ of the upper level and the frequency of doublet splitting δ. This has revealed a number of interesting regularities in the temporal dynamics of the SR field and the atomic subsystem. Figure 2 shows a typical example of such calculations for $\delta \ll 1$ ($\omega_{21} \ll \Omega$). It can be seen that the real part of the SR electric field amplitude (Fig. 2b) exhibits temporal dynamics $\{\mathrm{Re}[\mathscr{E}(\tau)] \neq 0\}$, while its imaginary part (Fig. 2c) does not evolve in time ($\mathrm{Im}[\mathscr{E}(\tau)] = 0$). The real parts of the high-frequency coherences $\mathrm{Re}[\mathcal{R}_{31}(\tau)]$ (Fig. 2d) and $\mathrm{Re}[\mathcal{R}_{32}(\tau)]$ (Fig. 2m) behave identically, while their imaginary parts $\mathrm{Im}[\mathcal{R}_{31}(\tau)]$ (Fig. 2f) and $\mathrm{Im}[\mathcal{R}_{32}(\tau)]$ (Fig. 2n) exhibit the antiphase behavior. Accordingly, the squares of their moduli evolve identically, $|\mathcal{R}_{31}|^2 = |\mathcal{R}_{32}|^2$ (see Figs. 2d and 2l). The dynamics of populations $\rho_{11}(\tau)$ (Fig. 2g) and $\rho_{22}(\tau)$ (Fig. 2o) are identical and repeat the dynamics of the SR field intensity $|\mathscr{E}|^2$ (Fig. 2a). It should be noted that these regularities are the consequences of the initial conditions (7)–(9) and are realized for any physically realistic parameters α and δ. This allows us to considerably simplify the mathematical analysis of the problem under investigation.

We pay attention to the fact that the cooperative radiation signal represents a quasi-periodically (or chaotically) repeating comb of peaks (trains) with a characteristic repetition time on the order of the period $2\pi/\delta$ ($2\pi/\omega_{21}$) of the low-frequency coherence oscillations. This is due to the fact that for a nonzero doublet splitting ($\delta \neq 0$), states $|+\rangle$ and $|-\rangle$ are not stationary anymore because with time the bright state is periodically transformed to the dark state. The aperiodicity of train repetition is associated with the effect of population trapping [41] (a part of population of the lower level is trapped into the dark state that does not interact with the upper state). For a strong doublet splitting $\delta \gg 1$ ($\omega_{21} \gg \Omega$), the SR dynamics consists of periodically repeating peaks of duration Ω^{-1}, which are modulated with the doublet splitting frequency ω_{21} [41].

Here it is appropriate to distinguish between the standard Dicke SR and cooperative emission from an ensemble of three-level Λ radiators in a high-Q cavity considered here. Starting from the Dicke state, our system generally does not return to it, although may approach this state. The exceptions are the limits of a degenerate doublet ($\omega_{21} = 0$), a strongly nondegenerate doublet ($\omega_{21} \gg \Omega$) [41], and a quasi-periodic regime (for $\omega_{21} < \Omega$ and $\alpha = 1$). In the dynamic chaos regime (for $\omega_{21} \ll \Omega$ and $\alpha < 1$), the behavior of the system after its start is determined by the current state of the field and the system of emitters. The emission dynamics loses its "spontaneous" character. The phase portrait of the system in this case is an entangled open trajectory, and its spectrum resembles white noise (see Sections 5 and 6).

Introducing the notations

$$\mathrm{Re}[\mathscr{E}] = \epsilon, \quad \mathrm{Im}[\mathscr{E}] = 0, \quad \rho_{21} = \eta + i\chi, \tag{10a}$$

$$\rho_{11} = \rho_{22} = \frac{1-\rho_{33}}{2}, \quad \rho_{33} = \alpha - \epsilon^2, \tag{10b}$$

$$\begin{gathered} \mathrm{Re}[\mathcal{R}_{31}] = \mathrm{Re}[\mathcal{R}_{32}] = \xi, \\ \mathrm{Im}[\mathcal{R}_{31}] = -\mathrm{Im}[\mathcal{R}_{32}] = \zeta, \\ |\mathcal{R}_{31}|^2 = |\mathcal{R}_{32}|^2 = \xi^2 + \zeta^2, \end{gathered} \tag{10c}$$

we can transform the system of differential equations (4) into the following form:

$$\dot{\epsilon} = 2\xi, \tag{11a}$$

$$\dot{\xi} = \frac{\delta}{2}\zeta + \frac{1}{2}(3\alpha - 1)\epsilon - \frac{3}{2}\epsilon^3 - \epsilon\eta, \tag{11b}$$

$$\dot{\zeta} = -\frac{\delta}{2}\xi - \epsilon\chi, \tag{11c}$$

$$\dot{\eta} = \delta\chi + 2\epsilon\xi, \tag{11d}$$

$$\dot{\chi} = -\delta\eta + 2\epsilon\zeta. \tag{11e}$$

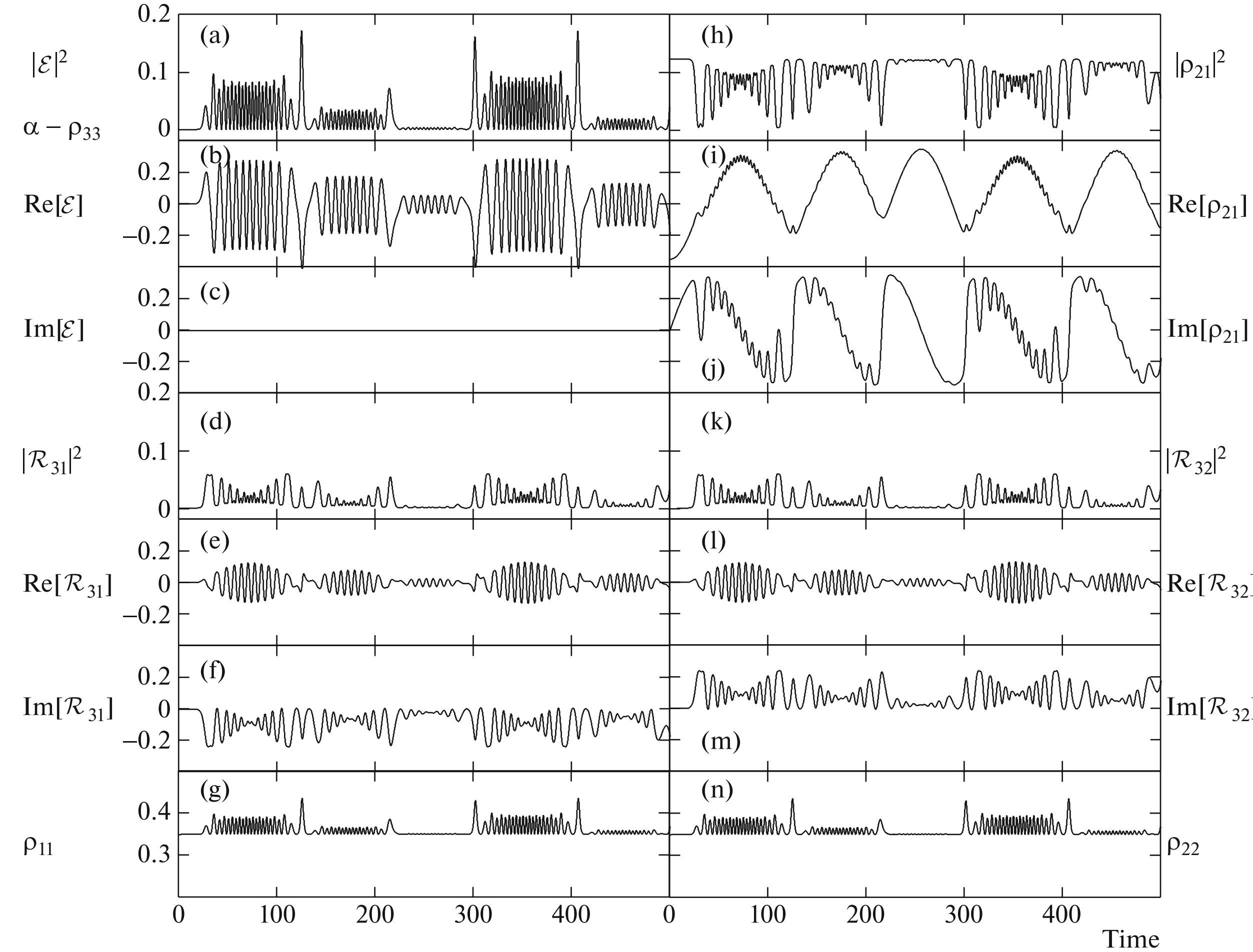

Fig. 2. Dynamics of the SR field strength $\mathcal{E}$, its intensity $|\mathcal{E}|^2$, and the density matrix elements ρ_{mn} of the Hamiltonian system, calculated for the doublet splitting $\delta = 0.05$ (in units of Ω) and the initial conditions $\rho_{33}(0) = \alpha = 0.3$; $\rho_{11}(0) = \rho_{22}(0) = 0.35$; $\mathrm{Re}[\rho_{21}] = -0.35$, $\mathrm{Im}[\rho_{21}] = 0$, $\mathrm{Re}[\mathcal{R}_{31}(0)] = \mathrm{Re}[\mathcal{R}_{32}(0)] = 10^{-8}$; $\mathrm{Re}[\mathcal{E}(0)] = \mathrm{Im}[\mathcal{E}(0)] = \mathrm{Im}[\mathcal{R}_{31}(0)] = \mathrm{Im}[\mathcal{R}_{32}(0)] = 0$. The time is measured in units of Ω^{-1}.

Therefore, the relations (10) ensure the reduction of our model from the complex-valued to the real-valued domain. As a consequence, the initial phase space $\mathbb{R}^{11}$ of the model (4) is fully mapped into $\mathbb{R}^5$ (11). In addition, taking into account the relations (5c) and (10), the integral of motion (5b) takes the form

$$\begin{gathered}\frac{3}{2}(\alpha - \epsilon^2)^2 - (\alpha - \epsilon^2) \\ +2(\eta^2 + \chi^2 + 2\xi^2 + 2\zeta^2) = \text{const}, \\ \text{const} = 2\alpha(\alpha - 1) + 4\mathcal{R}_0^2 + \frac{1}{2}.\end{gathered} \tag{12}$$

It should be emphasized that this conservation law limits the domain of phase trajectories of the system and determines a closed hypersurface in the phase space $(\epsilon, \xi, \zeta, \eta, \chi)$, outside of which the system of equations (11) has no solution for any values of parameters α and δ. This allows us to characterize the SR process as being stable in the Lagrange sense (see, for example, [60]). The canonical form of this hypersurface is defined by the equation

$$\begin{gathered}(\epsilon^2 - \gamma)^2 + \frac{4}{3}(\eta^2 + \chi^2 + 2\xi^2 + 2\zeta^2) = \text{const}, \\ \text{const} = \frac{4}{3}(\alpha^2 - \gamma + 2\mathcal{R}_0^2), \quad \gamma = \alpha - \frac{1}{3}.\end{gathered} \tag{13}$$

Its topological features depend on the sign of constant γ. For values $1/3 < \alpha \le 1$ (i.e., for $\gamma > 0$), this is a five-dimensional dumbbell with the symmetry axis ϵ. If $0 < \alpha \le 1/3$ (i.e., $\gamma < 0$), the hypersurface is a 5D ellipsoid.

4. STATIONARY POINTS

As mentioned above, the main object of our interest is a nondegenerate doublet ($\delta \neq 0$) because the model under investigation demonstrates nontrivial dynamics precisely in this case (see [43]). First of all, we determine its stationary points by equating to zero the derivatives in the system of differential equations (11). This gives

$$-\delta\eta + 2\epsilon\zeta = 0, \tag{14a}$$

$$\delta\zeta + (3\alpha - 1)\epsilon - 3\epsilon^3 - 2\epsilon\eta = 0, \tag{14b}$$

$$\xi = 0, \quad \chi = 0. \tag{14c}$$

This system of algebraic equations is not complete with respect to variables ϵ, η, ζ. Supplementing this system with the conservation law (12), we obtain the following closed equation for the SR electric field strength:

$$\frac{1}{2(4\epsilon^2 - \delta^2)^2}(a_0\epsilon^8 + a_1\epsilon^6 + a_2\epsilon^4 + a_3\epsilon^2 + a_4) = 0, \tag{15}$$

where a_i ($i = 0, 1, \ldots, 4$) are constants depending on the initial population α of the third level and splitting δ of the doublet. The first cofactor in Eq. (15) always differs from zero: $(1/2)(4\epsilon^2 - \delta^2)^{-2} \neq 0$. Then the polynomial in the numerator must be equal to zero:

$$U(\epsilon) = \epsilon^8 + b_1\epsilon^6 + b_2\epsilon^4 + b_3\epsilon^2 + b_4 = 0, \tag{16}$$

where $b_i = a_i/a_0$ can be expressed as

$$\begin{aligned} b_1 &= \frac{\delta^2}{4} - 2\alpha + \frac{2}{3}, \\ b_2 &= \frac{1}{192}[64\alpha(2\alpha - 1) + 32(1 - 3\alpha)\delta^2 + 3\delta^4], \\ b_3 &= \frac{\delta^2}{96}[\delta^2 - \alpha(3\delta^2 - 40\alpha + 32) + 8], \\ b_4 &= -\frac{\delta^4}{192}(\alpha - 1)^2. \end{aligned} \tag{17}$$

Having found the roots ϵ_n ($n = 1, 2, \ldots, 8$) of Eq. (16), we can determine all the remaining coordinates of stationary points ξ_n, ζ_n, η_n, χ_n of the phase space using relations (14):

$$\begin{aligned} \xi_n &= 0, \quad \chi_n = 0, \\ \eta_n &= \frac{2(\epsilon_n)^2[3(\epsilon_n)^2 - 3\alpha + 1]}{\delta^2 - 4(\epsilon_n)^2}, \\ \zeta_n &= \frac{\delta\epsilon_n[3(\epsilon_n)^2 - 3\alpha + 1]}{\delta^2 - 4(\epsilon_n)^2}. \end{aligned} \tag{18}$$

It should be noted that Eq. (16) contains only the terms with even powers of ϵ. A simple substitution $I = \epsilon^2$ reduces this equation to the fourth-power equation

$$I^4 + b_1I^3 + b_2I^2 + b_3I + b_4 = 0,$$

whose solution can be found, for example, by the standard Ferrari method [61]. This equation has four different roots, while in the sought variable ϵ, it has eight pairwise symmetric real-valued and pairwise conjugate complex-valued roots which, with allowance for relations (18), give the complete set of coordinates of the stationary points $A_n = (\epsilon_n, \xi_n, \zeta_n, \eta_n, \chi_n)$:

$$\begin{aligned} \epsilon_{1,2} &= \mp\frac{1}{4\sqrt{3}}\sqrt{Q_1 - \sqrt{D_1}}, \\ \zeta_{1,2} &= -\frac{\epsilon_{1,2}}{24\delta}(G_1 + \sqrt{D_1}), \\ \eta_{1,2} &= \frac{1}{96}(S_1 + \sqrt{D_1}), \\ \xi_{1,2} &= 0, \quad \chi_{1,2} = 0, \end{aligned} \tag{19}$$

$$\begin{aligned} \epsilon_{3,4} &= \mp\frac{1}{4\sqrt{3}}\sqrt{Q_1 + \sqrt{D_1}}, \\ \zeta_{3,4} &= -\frac{\epsilon_{3,4}}{24\delta}(G_1 - \sqrt{D_1}), \\ \eta_{3,4} &= \frac{1}{96}(S_1 - \sqrt{D_1}), \\ \xi_{3,4} &= 0, \quad \chi_{3,4} = 0, \end{aligned} \tag{20}$$

$$\begin{aligned} \epsilon_{5,6} &= \mp\frac{1}{4\sqrt{3}}\sqrt{Q_2 - \sqrt{D_2}}, \\ \zeta_{5,6} &= -\frac{\epsilon_{5,6}}{24\delta}(G_2 + \sqrt{D_2}), \\ \eta_{5,6} &= \frac{1}{96}(S_2 + \sqrt{D_2}), \\ \xi_{5,6} &= 0, \quad \chi_{5,6} = 0, \end{aligned} \tag{21}$$

$$\begin{aligned} \epsilon_{7,8} &= \mp\frac{1}{4\sqrt{3}}\sqrt{Q_2 + \sqrt{D_2}}, \\ \zeta_{7,8} &= -\frac{\epsilon_{7,8}}{24\delta}(G_2 - \sqrt{D_2}), \\ \eta_{7,8} &= \frac{1}{96}(S_2 - \sqrt{D_2}), \\ \xi_{7,8} &= 0, \quad \chi_{7,8} = 0. \end{aligned} \tag{22}$$

Here, the constants $Q_{1,2}$ and $D_{1,2}$, $G_{1,2}$, and $S_{1,2}$ have the form

$$\begin{aligned} Q_{1,2} &= 24\alpha - 8 \pm 8\kappa - 3\delta^2, \\ \kappa &= \sqrt{1 + 3(\alpha - 1)\alpha}, \end{aligned} \tag{23}$$

$$\begin{aligned} D_1 = {} & 768\alpha^2 - 128(\kappa - 1) - 48(5\kappa + 1)\delta^2 \\ & + 9\delta^4 + 48\alpha(8\kappa + 3\delta^2 - 12), \end{aligned} \tag{24}$$

$$\begin{aligned} D_2 = {} & 768\alpha^2 + 128(\kappa + 1) + 48(5\kappa - 1)\delta^2 \\ & + 9\delta^4 - 48\alpha(8\kappa - 3\delta^2 + 12), \\ G_{1,2} &= 24\alpha - 8 \pm 8\kappa + 3\delta^2, \\ S_{1,2} &= 24\alpha - 8 \mp 40\kappa + 3\delta^2. \end{aligned} \tag{25}$$

We are interested in the solutions to the problem under investigation only in the real domain. All coordinates (19)–(22) of stationary points A_n determined above are functions of parameters α and δ; therefore, it is important to find their values for which ϵ_n, ξ_n, ζ_n, η_n, and χ_n are real numbers. This is required for the radicands in the expressions (19)–(22) to be greater than or equal to zero:

$$D_{1,2} \geq 0, \quad H^{\mp}_{1,2} = (Q_{1,2} \mp \sqrt{D_{1,2}}) \geq 0. \tag{26}$$

Not going into details of the analysis, we only note that the stationary points $A_{1,2,3,4}$ exist in a part of two-parametric domain (α, δ), in which $H_1(\alpha, \delta) \geq 0$. This domain of existence of solutions (19) and (20) is bounded by the lower branch of the zero equipotential level $D_1(\alpha, \delta) = 0$ (24) and is defined by the inequality

$$\delta \leq \frac{2}{\sqrt{3}}\sqrt{2 - 6\alpha + 10\kappa - 4\sqrt{3}\sqrt{2 + \kappa - 3\alpha(2 - 2\alpha + \kappa)}}.$$

The singular points $A_{5,6}$ defined in (21) do not exist since $H_2^-(\alpha, \delta) \leq 0$ for the entire range of parameters (α, δ). Conversely, the points $A_{7,8}$ defined in (22) always exist because $H_2^+(\alpha, \delta) \geq 0$ for any (α, δ).

Let us return to the polynomial $U(\epsilon) = \epsilon^8 + b_1\epsilon^6 + b_2\epsilon^4 + b_3\epsilon^2 + b_4$ (16). As noted above, its zeros determine in the phase space the systems stationary points (maxima, minima, and so on). Only the real zeros have physical meaning. Their existence and number depends on the initial population α of the upper level and the doublet splitting δ. The remaining (nonphysical) zeros are pairwise conjugate complex numbers. The change in the number of real zeros and their multiplicity indicates a change in the number of stationary points in the phase space of the system, which substantially affects the SR dynamics, leading to bifurcation of the system upon a transition through certain critical values α_{cr} and δ_{cr} (see below).

Figure 3 shows the polynomial $U(\epsilon)$ for a certain sampling of values α and δ. This figure illustrates the patterns of the number of zeros and their degeneracy and, hence, the number of stationary points of the system. For example, as follows from Fig. 3a, the polynomial $U(\epsilon)$ has six different roots for $\alpha = 0.48$ and $\delta = 0.6$, while for $\alpha = 0.6$ and $\delta = 1.65$ (Fig. 3e), there are two triply degenerate roots. Finally, for $\alpha = 0.48$ and $\delta = 1.8$, the polynomial has only two real-valued roots (Fig. 3f), while the remaining roots are complex-valued (unphysical). Arrows show the degenerate roots that determine the specific bifurcation transition.

Concluding the section, we note that the zeros become degenerate for certain critical values of α_{cr} and δ_{cr}, which determine a singular point (of bifurcation transition of the system) in the parameter's space (α, δ). The collection of such points in the (α, δ) space determine a line demarcating the domains of dynamic SR regimes, which is also an interesting trend in investigation; however, it will be the subject of a standalone study and is not considered here.

5. POINCARÉ MAPPING: STAGES OF THE SYSTEM RANDOMIZATION

The Poincaré mapping method is one of the effective tools for investigating the nonlinear (chaotic) dynamics of complex systems. In this section, we apply this method for our model presuming small doublet splitting $\delta \ll 1 \ll \Omega$. The essence of this method can be explained as follows [62]. We measure stroboscopically the dynamic variables and moments, corresponding to a certain phase ϕ of a moving phase point, with a certain period T. For obtaining a Poincaré map, we select a sampling of values of functions $\epsilon(\tau_n)$, $\xi(\tau_n)$, $\zeta(\tau_n)$, $\eta(\tau_n)$, and $\chi(\tau_n)$ ($n = 0, 1, 2, ...$) at the discrete instants $\tau_n = nT + \phi$. A variation of phase ϕ is equivalent to the rotation of the Poincaré plane (volume) by the corresponding angle. This method makes it possible to distinguish between periodic (quasi-periodic) and aperiodic (including chaotic) types of motion and to trace bifurcation processes (i.e., the processes of transition of the system under investigation to certain qualitatively new states). If the Poincaré map does not consist of a finite set of localized points or has no closed orbit (which corresponds to a quasi-periodic motion or "motion on a torus"), such motion may appear to be chaotic.

Figure 4 shows the results of numerical calculations of two (ϵ, ξ, η) and (ϵ, ξ, ζ) of ten 3D Poincaré maps with the stroboscopic sampling of values from the corresponding vectors (ϵ, ξ, ζ, η, χ) at instants $\tau_n = nT$, where period $T = \pi$ ($n = 0, 1, 2, ...$). In this case, we fix phase $\phi = 0$, which does not alter the topology of the phase volume.

In all Poincaré maps, the points indicate the positions of extrema or repulsion centers on a phase trajectory; the digits 7 and 8 label points in accordance with the notations adopted in Section 4. Figure 4 also shows the corresponding Fourier spectra of the field ϵ; each Fourier spectrum (except the upper one for $\alpha = 1$) contains an inset showing the cross-section of the Poincaré map (ϵ, ξ, ζ) by a plane parallel to the (ξ, ζ) plane and intersecting the ϵ axis at a point $\epsilon = 0.5$. Calculations were performed for different values of the initial population α of the third level (indicated in the figure) and a small fixed splitting $\delta = 0.05$ of the doublet. The remaining parameters of the calculations are given in the caption to Fig. 4.

By hypothesis, the model under investigation is conservative; the phase space of the model is stable in the Lagrange sense and bounded by the hypersurface (13) (see Section 2). In the SR regime with $1/2 < \alpha \leq 1$, this hypersurface is represented topologically by a dumbbell with a narrow waist in the vicinity of the singular point located at the origin. This point is the separatrix and a center of strong attraction as well as repulsion of the mapping phase point upon its moving off and approaching, respectively.

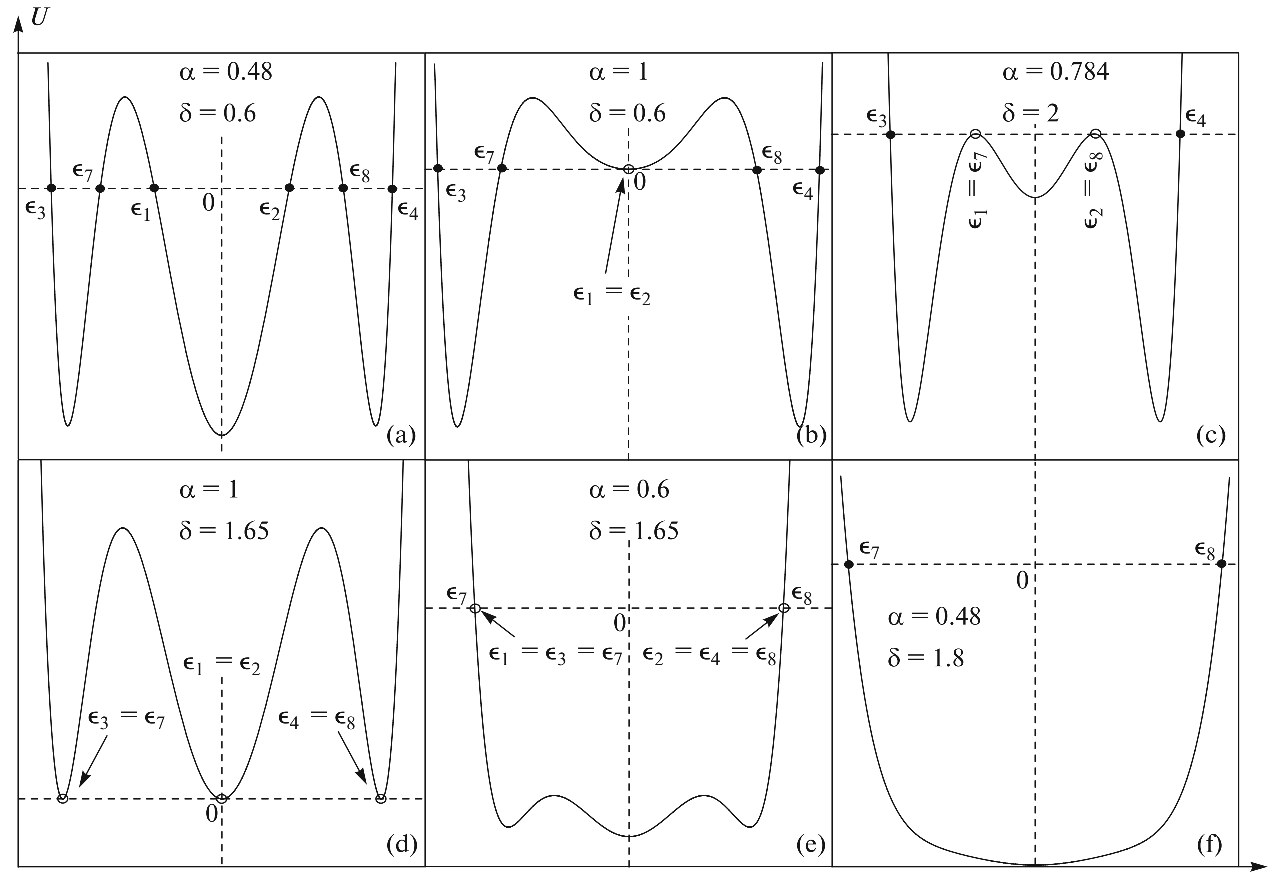

Fig. 3. Plots of the polynomial $U(\epsilon) = \epsilon^8 + b_1\epsilon^6 + b_2\epsilon^4 + b_3\epsilon^2 + b_4$ (16) whose zeros (that determine stationary points of the system) can be degenerate for a certain sampling of critical values α_{cr} and δ_{cr}. The dashed lines show the coordinate axes; the dark circles indicate the nondegenerate roots of the polynomial $U(\epsilon)$; the light circles denote degenerate roots. The rot multiplicity is explicitly shown by equating the corresponding roots ϵ_n. The arrows point the degenerate roots that determine a specific bifurcation transition.

When the system passes from the SR regime to the SR regime without inversion, that occurs for $\alpha = 1/2$, the waist of the dumbbell is broadened substantially, and the dumbbells is transformed into an ellipsoid even for $\alpha = 1/3$. For this reason, depending on parameter α, we will henceforth speak of the motion in the phase space over tori in the inner cavity of the dumbbell ($1/2 < \alpha < 1$), or over tori lying on the dumbbell surface, when $\alpha = 1/2 + 0^+$, or over a large number of tori lying in the inner region of the ellipsoid ($\alpha < 1/3$).

It can be seen from Fig. 4 that for the initial population $\alpha = 1$ of the third level, the Poincaré maps are closed curves that never pass through the origin (separatrix) [45]. The fact that the curves in Poincaré maps are closed indicates quasi-periodicity of the given motion or the motion of the representative point over the surfaces of two five-dimensional tori, lying in the left (right) cavity of the dumbbell. The quasi-periodicity of motion is confirmed by the Fourier spectrum of the field ϵ (see Fig. 4, $\alpha = 1$). Predominant spikes can be seen at frequencies multiple of the frequency $f_0 = f_2 - f_1 = \pi/10$, where $f_k = (k - 1/2)f_0$, $k = 1, 2, \ldots$. This result corresponds, to a high degree of accuracy, to the Kolmogorov–Arnold–Moser conditions of quasi-periodicity of oscillations (see, for example, [63]).

As a result of an insignificant decrease in the population ($\alpha = 0.99$) of the third level (see the corresponding curve in Fig. 4), the closed trajectory in Poincaré maps (see the previous case with $\alpha = 1$) is transformed into two tori lying in the cavities of the dumbbell; this can clearly be seen on the (ϵ, ξ, ζ) map and in the corresponding inset. To demonstrate the peculiarities of these tori, the inset shows a cut by the (ξ, ζ) plane on a magnified scale indicated in the octant I. The Fourier spectrum of the field displays the presence of small-amplitude subharmonics in the vicinity of frequencies f_k.

For $\alpha = 0.7$ (see the corresponding diagram in Fig. 4), the tori are broadened and turn inside out, dif-

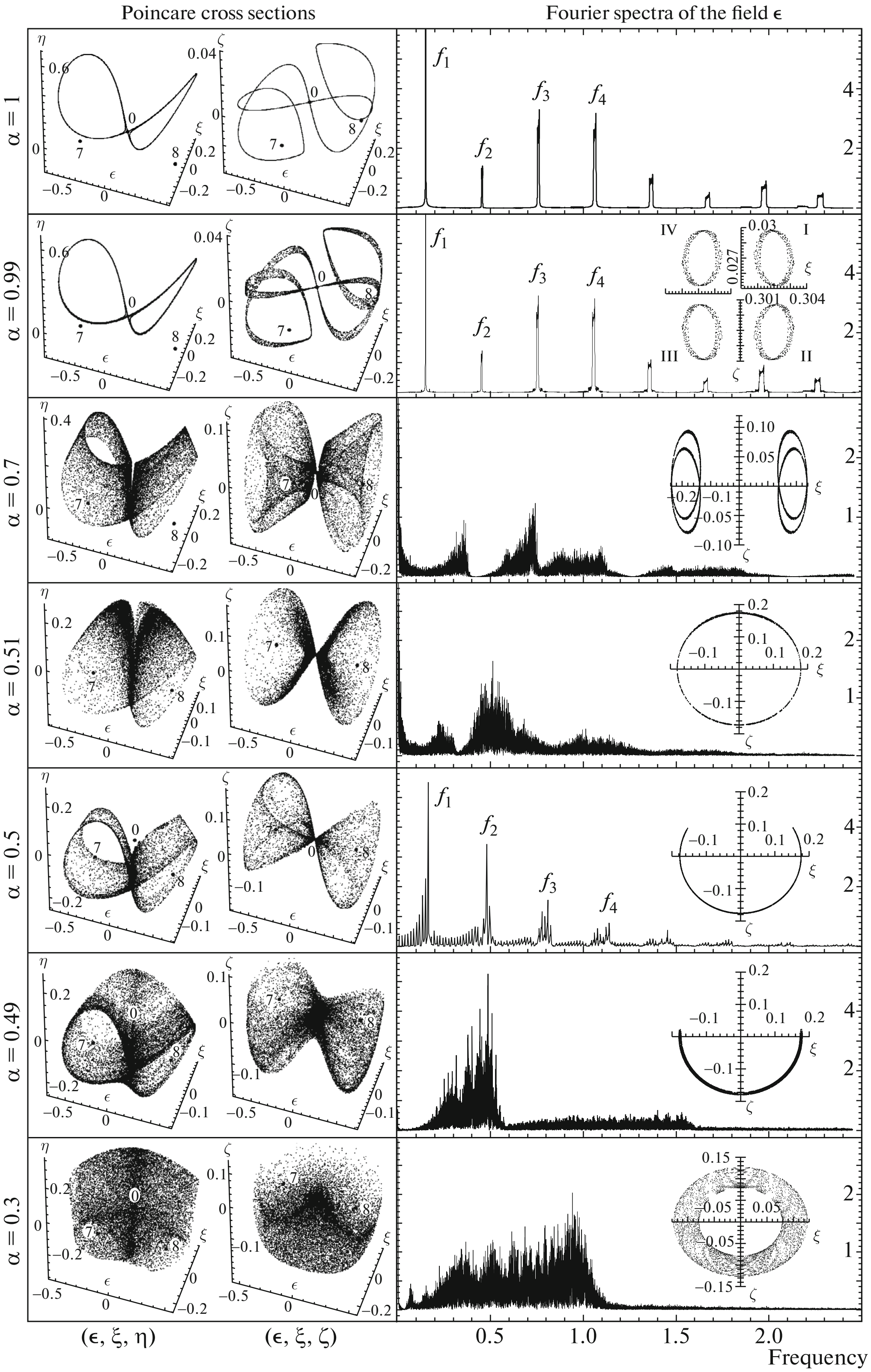

Fig. 4. An example of two of ten 3D Poincaré maps and the Fourier spectrum of the SR field strength ϵ, depending on $\rho_{33}(0) = \alpha$ (shown on the left), which were obtained by numerical solution of Eqs. (11) with the initial conditions $\epsilon(0) = 0$, $\eta(0) = (\alpha - 1)/2$, $\chi(0) = 0$, $\xi(0) = \mathcal{R}_0 = 10^{-8}$; $\zeta(0) = 0$. The doublet splitting is $\delta = 0.05$ (in units of Ω). Frequency is given in units of Ω.

fusing into themselves within the dumbbell surface. The beginning of diffusion of parts of tori into themselves is precisely the instant of the beginning of a transition of the system from the quasi-periodic motion to chaos. It is important to note in this connection that the phase trajectories at the instant of turning inside out do not intersect one another, forming a heteroclinic structure (see, for example, [64]). In this case, the Fourier spectrum of the field does not resemble any longer a set of certain harmonics. It rather resembles a noise spectrum. This means that for $\alpha = 0.7$, the system is in the state of dynamic chaos.

The degree of randomization of the processes occurring in the system under investigation increases upon a further decrease in the population of the third level to $\alpha \to 1/2$. As a result, the Fourier spectrum becomes noisier (the corresponding graph in Fig. 4 corresponds to $\alpha = 0.51$). The initial tori have turned inside out completely and represent parts of the dumbbell surface (left or right). The representative point moves over the dumbbell surface (excluding the origin), which in turn is covered by the phase trajectory almost completely. In this case, the representative vector, following the representative point over the dumbbell, surface changes its length unpredictably, bringing the system to dynamic chaos.

It should be noted that, upon a transition from the SR regime to the SR regime without inversion on the interval $1/3 < \alpha < 1/2$, the 5D dumbbell is transformed into a 5D ellipsoid (see Section 2). In this case, the physical properties of SR radically change: the point $\alpha = 1/2$ is a bifurcation (transient) point between the SR regime and the inversionless SR regime. This instant of the transition is characterized by a high degree of quasi-periodicity, which is manifested itself in the corresponding Fourier spectrum of the field by the presence of stable harmonics at frequencies $f_k = (k - 1/2)f_0$ and subharmonics at frequencies multiple of $f_k/20$.

As a result of bifurcation, the system passes to a new type of chaos, for which the system's state is characterized by a broad structureless spectrum (see Fig. 4, $\alpha = 0.49$). The representative vector, which changes its length unpredictably, follows the representative point not only over the dumbbell surface, but also in a certain neighborhood under it (see the inset to the corresponding panel).

Upon a further decrease of the parameter α (see Fig. 4, $\alpha = 0.3$), the observed randomization of the dynamic system becomes stronger. After passing through the boundary value $\alpha = 1/3$, the initial phase space of the dumbbell-type model is completely transformed into an ellipsoid. The Fourier spectrum of the field is characterized by the absence of well defined harmonics and resembles white noise. The corresponding inset in this panel indicates the presence of a broad zone of random walk of the phase point representative vector under the surface of the ellipsoid.

6. MECHANISM AND SCENARIOS OF DYNAMIC CHAOS

Let us consider the dynamics of evolution of the system under investigation in the case when the spectrum of the SR field is substantially noise-polluted (see Fig. 4 in Section 5). The characteristic conditions of such regimes can be described as follows: (i) a domain of the SR regime in the vicinity and above the bifurcation transition of the system to the SR state without inversion ($\alpha = 1/2 + 0^+$), in which the phase trajectory lies on the surface of the dumbbell; (ii) a domain of the inversionless SR regime ($0 < \alpha < 1/2$), in which the bridge between the dumbbell cavities expands and ensures the condition for wandering of the phase trajectory within the hypersurface (13).

It should be noted that the dimension of the phase space in the case of a degenerate doublet ($\delta = 0$) is $\mathbb{R}^2$ [45]. Even an infinitesimal splitting of the doublet transforms its dimension stepwise from $\mathbb{R}^2$ to $\mathbb{R}^5$ and is responsible for a complex behavior of the system's representative point in the phase space ($\epsilon, \xi, \zeta, \eta, \chi$) (see Fig. 4 in Section 5). Actually, this can be seen from the system of equations (11) after its certain transformation. For this purpose, we introduce new functions ε, ϑ, and ϱ by the relations

$$\varepsilon = \frac{1}{2}\epsilon, \quad \eta = \delta\vartheta + 2\varepsilon^2 + \frac{1}{2}(\alpha - 1), \quad \zeta = \varrho - 2\varepsilon\vartheta. \tag{27}$$

This gives the following system of differential equations equivalent to the initial system:

$$\dot{\varepsilon} = \xi, \tag{28a}$$

$$\dot{\xi} = 2\alpha\varepsilon - 16\varepsilon^3 + \frac{1}{2}\delta\varrho - 3\delta\vartheta\varepsilon, \tag{28b}$$

$$\dot{\varrho} = -\frac{1}{2}\delta\xi + 2\xi\vartheta, \tag{28c}$$

$$\dot{\vartheta} = \chi, \tag{28d}$$

$$\dot{\chi} = 4\varrho\varepsilon - 8\vartheta\varepsilon^2 - \delta^2\vartheta - 2\delta\varepsilon^2. \tag{28e}$$

For $\delta = 0$ (degenerate doublet), this system of equations splits into two independent blocks: Eqs. (28a) and (28b) for ε and ξ and Eqs. (28c)–(28e) for the remaining variables ϱ, ϑ, and χ. We are interested in the equation for the field, which in this limit has the form

$$\ddot{\varepsilon} - 2\alpha\varepsilon + 16\varepsilon^3 = 0 \tag{29}$$

and represents the well-known Duffing equation [65]. It has an analytic solution in terms of the Jacobi elliptic functions, which describes periodic pulsations of the SR field of a duration Ω^{-1} and of a period $T_D = 4\Omega^{-1}K(m)$, where $K(m)$ is the complete elliptic integral of the first kind. The parameter m is defined by the expression

$$m^2 = 1 - \frac{2\mathcal{R}_0^2}{4\mathcal{R}_0^2 + \alpha(\alpha/2 + \sqrt{\alpha^2/4 + 2\mathcal{R}_0^2})}$$

(see [45] for details). In this case, phase trajectories of the system in the $(\varepsilon, \dot{\varepsilon})$ space are always closed.

In the case of a nondegenerate doublet ($\delta \neq 0$), Eqs. (28) form a system of five coupled nonlinear equations. The difference from the case of the degenerate doublet ($\delta = 0$) consists in the presence of small (in parameter $\delta \ll 1$) anharmonic perturbations of the SR field by the atomic subsystem. These perturbations introduce disbalance into the Duffing oscillations of the SR field and ultimately bring the vibrational system to the intrinsic resonances and dynamic chaos [62–64, 66].

Let us consider the mechanism of randomization of the system. The representative point of the system evolving in time can substantially approach the separatrix solution (origin of coordinates; see Fig. 5). In this case, the phase velocity of the representative point decreases almost to zero, and the system under investigation practically does not generate the SR field. At this instant, the conditions for outgoing (jump) of the phase trajectory to a new one occur. In the regime of the standard SR, this is the left or right cavity of the dumbbell (for example, the case of $\alpha = 1/2 + 0^+$ that corresponds to numerical calculations with the initial conditions $\alpha = 0.51$, $\delta = 0.05$, $\varepsilon(0) = 0$, $\vartheta(0) = (\alpha - 1)/(2\delta)$, $\chi(0) = 0$, $\xi(0) = \mathcal{R}_0 = 10^{-3}$, and $\varrho(0) = 0$ (see Figs. 5a and 5b). In the regime of SR without inversion, these are tori lying "under the hypersurface" (13), the case when $0 < \alpha < 1/2$ that corresponds to numerical calculation with the initial conditions $\alpha = 0.3$, $\delta = 0.055$, $\varepsilon(0) = 0$, $\vartheta(0) = (\alpha - 1)/(2\delta)$, $\chi(0) = 0$, and $\xi(0) = \mathcal{R}_0 = 10^{-4}$, and $\varrho(0) = 0$ (see Figs. 5c and 5d). In this case, the system arrives at dynamic chaos in accordance with the same scenario (distracting tori). The results of numerical calculations shown in Fig. 5 visually illustrate this situation.

I. Regime of the standard SR ($\alpha = 0.51$, $\gamma = \alpha - 1.3 > 0$, see Figs. 5a and 5b) is characterized by a complex motion of the phase point of the system over the surface of the dumbbell and by a noisy spectrum of the field (see Fig. 4, the Fourier spectrum for the corresponding value of α). The representative vector of the phase point of the system moves either in the region of the left branch of the dumbbell (we denote this motion by Θ_1) or "jumps" to the region of the right branch of the dumbbell (Θ_2, Fig. 5b). The dynamics of the electric field strength ε is completely consistent with such a behavior (see Fig. 5a). The motion in domain Θ_1 corresponds to the field oscillations in the positive half-plane (octant I), while the motion in domain Θ_2 corresponds to the field oscillations in the negative half-plane (octant II). The periods of time T_i ($i = 1, 2, \ldots$) in which the system is in domains Θ_1 and Θ_2 are essentially different. The difference also exists in the number of rotations performed by the representative vector moving in these domains of the phase space. For example, period T_7 (domain Θ_1) corresponds to 35 rotations of different amplitudes, while period T_8 (domain Θ_2) corresponds to 34 rotations also with different amplitudes. Any approach of the representative phase point to the separatrix creates new conditions in the evolution of the system (i.e., a new torus with completely different amplitude and frequency characteristics).

II. Regime of SR without inversion, $0 < \alpha \leq 1/3$ and $\gamma = \alpha - 1/3 < 0$ (see Figs. 5c and 5d), is also characterized by complex phase movements, but now in the bulk of the ellipsoid. Like in the previous case, the representative point of the system approaches the coordinate origin (separatrix) in certain time intervals. Each approach is accompanied with the destruction of the previous motion and a transition of the system to a qualitatively new state. In the phase space, this regime is a family of tori disintegrating with time [64]. Figure 5d shows the dynamics of evolution and distraction of the first two tori, as well as a graph of the SR electric field strength ϵ corresponding to this case (see Fig. 5c). The SR regime for these parameters of the system is unpredictable, that means dynamic chaos.

7. EFFECTS OF RELAXATION AND CAVITY LOSSES

The results described in Sections 3–6 were obtained for a Hamiltonian system (i.e., disregarding the cavity losses as well as homogeneous and inhomogeneous broadening in the system of emitters). It should be noted, however, that these processes are attributive features of actual systems. For this reason, it is important to discuss their effects on the inversionless SR regimes in the cavity discovered in this work. Since the realization of a specific scenario strongly depends on the initial population of the upper level and the doublet splitting, we will restrict our analysis to a set of parameters specified in Fig. 2, but now we will use the general equations (4), taking into account the cavity losses and relaxation in the system of emitters.

7.1. Cavity Losses

We assume that the relaxation times T_1, T_2, and T_2^* of the system of emitters are longer than the lifetime $T_{\rm res}$ of the field in the cavity, so that the latter process is a dominating channel of the SR field damping. In this case, the conservation law (5a) does not hold because the field leaves the cavity. One can expect that the inversionless SR regime found for an ideal system is also partly preserved in these conditions if its char-

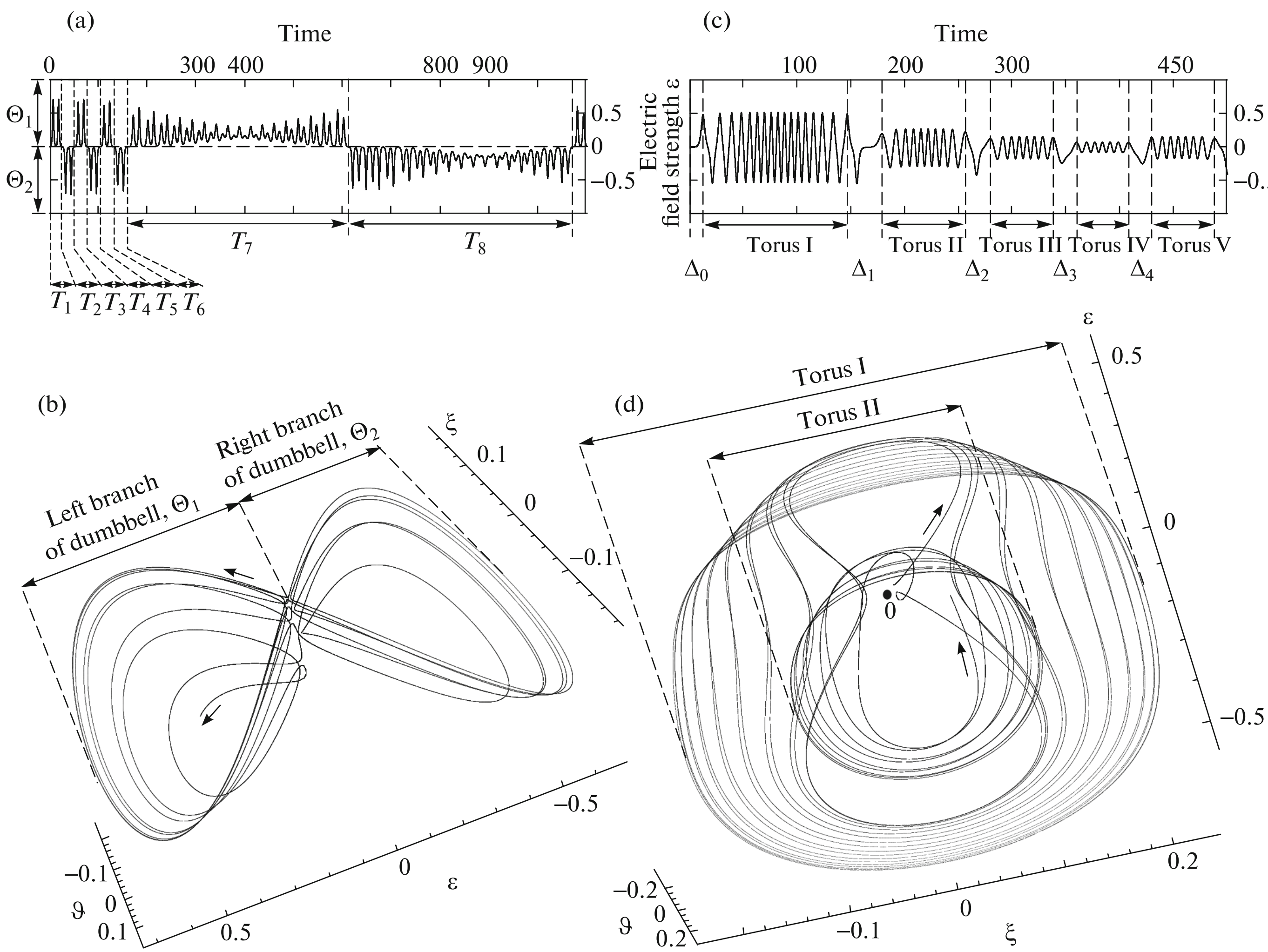

Fig. 5. (a, c) SR pulses and (b, d) phase portraits in the subspace (ε, ξ, ϑ) of the system, illustrating the emergence of chaos in it; (a, b) regime of the standard SR; (c, d) regime of SR without inversion. Calculations were performed on the basis of numerical integration of the system of equations (28) for the following conditions: (a, b) $\alpha = 0.51$; $\varepsilon(0) = 0$; $\vartheta(0) = (\alpha - 1)/2\delta$, $\chi(0) = 0$, $\xi(0) = \mathcal{R}_0 = 10^{-3}$, $\varrho(0) = 0$, $\delta = 0.05$; (c, d) $\alpha = 0.3$; $\varepsilon(0) = 0$; $\vartheta(0) = (\alpha - 1)/2\delta$, $\chi(0) = 0$, $\xi(0) = \mathcal{R}_0 = 10^{-4}$, $\varrho(0) = 0$, $\delta = 0.055$. The doublet splitting δ is given in units of Ω; time is measured in units of Ω^{-1}.

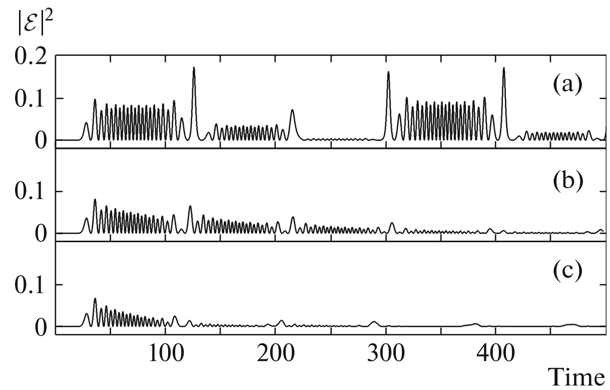

Fig. 6. Effect of cavity losses on the SR dynamics from the results of calculations based on the system of equations (4), disregarding the homogeneous and inhomogeneous broadening. The SR lifetime in the cavity is $\tau_{res} = \infty$ (a), 100 (b), and 50 (c) (in units of Ω^{-1}). The remaining parameters are the same as in Fig. 3. Time is measured in units of Ω^{-1}.

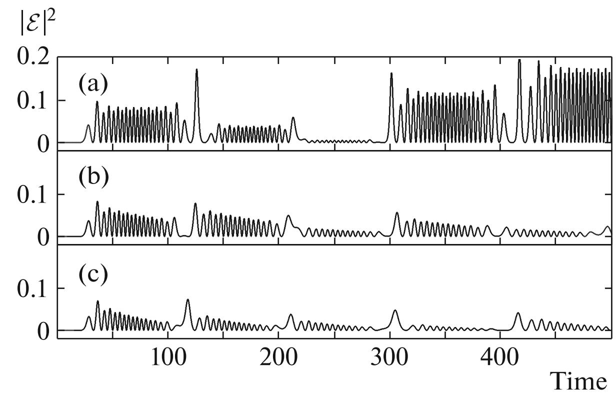

Fig. 7. Effect of homogeneous broadening on the SR dynamics from the results of calculations based on the system of equations (4), disregarding the cavity losses and inhomogeneous broadening. The coherence relaxation time $\tau_2 = 10^5$ (a), 100 (b), and 50 (c) (in units of Ω^{-1}). The population relaxation time $\tau_1 = 10^5$. The remaining parameters are the same as in Fig. 3. Time is measured in the units of Ω^{-1}.

acteristic time is shorter than T_{res}. Figures 6b and 6c show the results of calculations of the inversionless SR dynamics for various values of T_{res}, which confirms the above arguments. Indeed, the SR pulse in Figs. 6b and 6c preserves the features of the ideal case (see Fig. 6a) for $t < T_{res}$ and decreases when $t > T_{res}$.

7.2. Homogeneous Broadening

Let us now consider the effect of homogeneous broadening of optical transitions on the dynamics of three-level SR in the cavity, which is described by the times T_1 and T_2 (T_1 and T_2 processes). The homogeneous broadening causes relaxation of the coherence of each emitter with time T_2. In an open system, this leads to a monotonic decrease of the SR signal upon shortening T_2 and, as a consequence, to its complete vanishing [67, 68]. In our case, T_1 and T_2 processes lead to violation of the conservation laws (5b) and (5c). The system of emitters loses coherence, and the SR field decreases even in the absence of cavity losses. The population relaxation time T_1 is fixed (spontaneous decay) and is large on the SR scale, while the time T_2 depends on temperature and can be much smaller than T_1 and comparable with the SR lifetime. For this reason, in our analysis we fixed T_1 and varied T_2. The results of calculations are shown in Fig. 7. As is seen, the global effect of homogeneous broadening consists in suppression of SR and a change in its time scale upon decreasing T_2. At first glance, it is surprising that the signal exists over time intervals considerably exceeding T_2. We attribute this to the low-frequency coherence ρ_{21}, which does not decay in our model (see Eq. (4c)) and represents therefore a source of the high-frequency coherence (see Eqs. (4d) and (4e)). Recall that we disregard the cavity losses in this case. This means that the field does not escape from the system, but it decreases due to dephasing. These two factors lead to a partial revival of the SR signal for times $t > T_2$. It should also be noted that even for short T_2, the SR pulse exhibits quasi-periodicity that approximately corresponds to the period $2\pi/\omega_{21}$ of oscillations of the low-frequency coherence, but it nevertheless decays with time. Thus, in spite of some peculiarities in the effect of homogeneous broadening on the cavity inversionless SR, it ultimately destroys the regime of the Hamiltonian system for $t > T_2$.

7.3. Inhomogeneous Broadening

Let us consider the effect of inhomogeneous broadening on the dynamics of cooperative three-level emission in a cavity, assuming that all remaining relaxation times are much longer. This type of broadening violates the conservation law (5c). In the general case, inhomogeneous broadening differs significantly from its homogeneous counterpart: the phase of each emitter is preserved, and only the collective response decreases with time (in the linear case). The phases of the emitters can, in principle, be inverted using a coherent pulse, and a photon echo signal can be observed in this case (see, for example, [69]). For this reason, this type of relaxation is often referred to as reversible relaxation. In the case of an open system, inhomogeneous broadening, in the same manner as homogeneous one, suppresses the SR signal [67, 68]. If, however, the Q factor of the cavity containing the system is high enough (i.e., the SR field is retaining in the cavity for a long time), quasi-periodic (or even chaotically repeating) combs of the SR pulses (like in our case) play the role of coherent trains, inverting the phases of emitters. It can then be expected that the effect of inhomogeneous broadening on SR radically differs from the effect of homogeneous broadening, that is actually the case. Figure 8 shows the corresponding results of calculations of the inversionless SR dynamics, modeling the inhomogeneous contours $g_{31}(\omega)$ and $g_{32}(\omega)$ by identical Gaussian distributions with the standard deviation T_2^{*-1} (T_2^* is the inhomogeneous relaxation time) for different values of T_2^*. As is seen from Fig. 8, even a significantly large (on the computation scale) time T_2^* leads to a noticeable change in the shape of the SR pulse obtained for an ideal (Hamiltonian) system (Fig. 8a). We attribute such a strong effect of even a small inhomogeneous broadening on the SR pulse to the fact that the system resides at the state of dynamic chaos already in the ideal (Hamiltonian) case. Therefore, even small variations in the emitters' phases during emission lead to an essentially different scenario of the system's optical dynamics, preserving, however, its chaotic nature. For shorter times T_2^*, the dynamics of SR without inversion experiences still stronger changes, but (which is important) exhibits no decay.

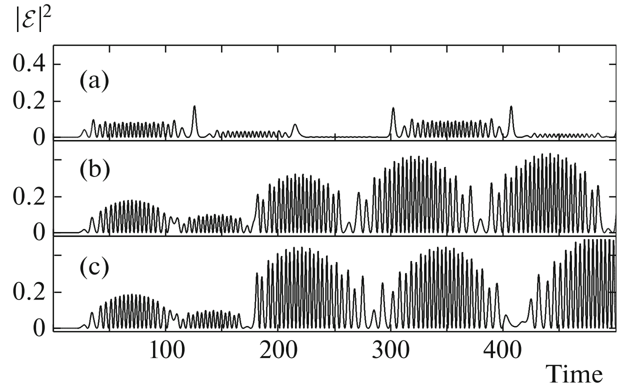

Fig. 8. Effect of inhomogeneous broadening on the SR dynamics from the results of calculations based on the system of equations (4) disregarding the cavity losses and homogeneous broadenings. The inhomogeneous relaxation time is $\tau_2^* = \infty$ (a), 1000 (b), and 100 (c) (in units of Ω^{-1}). The remaining parameters are the same as in Fig. 3. Time is measured in units of Ω^{-1}.

8. PROMISING SYSTEMS

Crystals doped with rare-earth ions (e.g., $LaF_3:Pt^{3+}$, $Y_2SiO_5:Pr^{3+}$, $Y_2SiO_5:Eu^{3+}$, and others) are the real objects in which the conditions for the observation of the nonstandard regimes of inversionless cavity SR can be realized. At cryogenic temperatures, the states of the 4*f* orbital of these ions exhibit a high degree of optical coherence (smaller than a kilohertz as in $Y_2SiO_5:Er^{3+}$ [70]) and a record-low inhomogeneous broadening (from megahertz to gigahertz) [70]. The coherence time of Zeeman or hyperfine states of the ground level may reach 6 hours [71]. The above extraordinary properties render the crystals doped with rare-earth ions to be very prospective systems from the viewpoint of solid-state optical memory and fully optical data processing [72], as well as for the observation of coherent optical effects (in particular, superradiance) [14, 15, 56, 73–79].

Below, we will use the optical parameters of rare-earth systems without mentioning a specific crystal. The lifetime T_1 of the states of the 4*f* orbital of rare-earth ions depends on the matrix and can vary from a few tens of microseconds to hundreds of milliseconds [70] (optical transitions in isolated ions are dipole-forbidden). For estimates, we choose T_1 ~ 10–100 ms. The SR time scale is determined by the cooperative frequency $\Omega = (2\pi d^2\omega N/\hbar)^{1/2}$, where the ion concentration N is a significant variable parameter. The transition dipole moment d can be determined from the lifetime T_1 of the excited state: $1/T_1 = 4d^2\omega^3 n/(3\hbar c^3)$, where n is the refractive index of the matrix (its typical value is $n \approx 1.6$). As a result, we obtain $\Omega^2 = 3c\lambda^2N/(8\pi T_1)$, whence $\Omega^2 \approx (10^2–4 \times 10^3)N$ cm^3 s^{-2} for $\lambda \approx$ 500–1000 nm and $T_1 \approx$ 10–100 ms. For the concentration $N \sim 10^{12}$ cm^{-3} of rare-earth ions, the cooperative frequency Ω is estimated as $\Omega \sim (1–5) \times 10^7$ s^{-1} and, accordingly, $\Omega^{-1} \approx (2–10) \times 10^{-8}$ s. The delay time of the SR pulse for the parameters of our calculations is $T_D \approx 25\Omega^{-1}$ (see Fig. 3), which gives $T_D \approx (0.25–2.5)$ μs for the above range of parameters. The population of the upper state below 0.5 can be attained by an incoherent pumping of submicrosecond duration. A typical scale of the hyperfine structure of the ground state of (non-Kramers) ions is on the order of 10–100 MHz, so that the coherence in the subsystem of these states can be produced by a pulsed microwave field of submicrosecond duration. As noted above, the optical coherence times T_2 in the aforementioned rare-earth systems belong to the millisecond range, while the inhomogeneous relaxation times T_2^* are in the submillisecond range.

According to the above estimates, the conditions for the observation of the cavity inversionless SR and its nonstandard regimes found in this work can be realized in the aforementioned systems. Indeed, for that to happen, first, the inequality $\Omega > \omega_{21}$ must be satisfied that can be met. Next, the system is required to be excited to the upper level, and the low-frequency coherence must be produced over a time interval shorter than the SR delay time T_D; this condition can also be realized. And finally, for initiating SR, an initial polarization must be induced by a coherent optical pulse of a small area and a duration shorter than T_D, that can be easily achieved. The trigger pulse should be directed at an angle to the system's axis to generate a wave propagating in one direction. As regards the homogeneous and inhomogeneous relaxation times T_2 and T_2^*, their values are much greater than the period $2\pi/\omega_{21}$ of the low-frequency coherence, characteristic for the chaotic structure of the SR pulse. The cavity losses can be made negligibly low using high-quality mirrors.

9. CONCLUSIONS

In this work, we have investigated theoretically the Dicke SR in a system of three-level quantum emitters with a doublet in the ground state (Λ scheme of operating transitions), placed into a cyclic cavity. For the standard (two-level) SR, an initial population inversion is required. In a particular case of Λ emitters, this limitation is not compulsory: SR is possible even if the population of the upper level is smaller than the total population of the doublet (Dicke SR without inversion). This regime can be realized if the doublet has been prepared in a coherent state.

In the ideal case of a Hamiltonian system, in which the cavity losses and homogeneous and inhomogeneous relaxation in the emitter system are negligibly small, we have obtained the conservation laws that make it possible to substantially reduce the dimension of the phase space of the model ($\mathbb{R}^{11} \to \mathbb{R}^5$) and to use the methods of dynamics of nonlinear system for analyzing the cavity three-level SR under these conditions. For this purpose, we have used the Poincaré mapping technique. It has been shown that in the general case of a nondegenerate doublet, the temporal dynamics of SR without inversion demonstrates different regimes (such as self-oscillations and chaos) which are not typical for the standard Dicke SR. The realization of these regimes is controlled by the initial population of the upper level and the doublet splitting.

Analysis of the Hamiltonian system takes advantage the integrals of motion (5a)–(5c). Being a basis for studying stationary states of the system and its possible evolution, it cannot be used directly for determining the system's dynamics in the presence of homogeneous and inhomogeneous broadening in the system of emitters and cavity losses, which are factors violating a particular conservation law. From the theoretical point of view, the analysis of optical dynamics of the system under investigation in the presence of these factors is an open and complicated problem. One of the methods for its at least partial solution is numerical integration of the control equations and comparison of their solutions with the ideal (Hamiltonian) case. In this way, certain conclusions can be drawn concerning the optical dynamics of the system in the presence of relaxation and time intervals, on which the Hamiltonian limit can be observed.

Hewing to this strategy, we have found that the cavity losses and homogeneous broadening (irreversible relaxation) lead to damping of the SR signal of a Hamiltonian system over time intervals longer than the corresponding relaxation times T_{res} and T_2. In other words, the system preserves its Hamiltonian nature over time $t < T_{res}$, T_2. The effect of inhomogeneous broadening on the cavity three-level SR, in view of its reversible nature, is essentially different. First, this broadening does not lead to damping of the SR signal. Second, even a small variation of its value results in to a noticeable change in the SR pulse obtained for an ideal (Hamiltonian) system, preserving herewith its chaotic nature. This is an interesting question that requires a further investigation.

ACKNOWLEDGMENTS

The authors are grateful to V.I. Yukalov and A.M. Basharov for support of this research, V.V. Ovsyankin and V.S. Zapasskii for the discussion of spectroscopic properties of crystals with rare-earth ions, and to A.A. Grib, A.S. Troshin, and L.V. Zhukov for stimulating discussions.

This work was supported by the Russian Foundation for Basic Research (project no. 15-02-08369).

REFERENCES

1. R. H. Dicke, Phys. Rev. **93**, 99 (1954).
2. N. E. Rehler and J. H. Eberly, Phys. Rev. A **3**, 1735 (1971).
3. K. Bonifacio, P. Schwendimann, and F. Haake, Phys. Rev. A 4, 302 (1971), Phys. Rev. A **4**, 854 (1971).
4. I. V. Sokolov and E. D. Trifonov, Sov. Phys. JETP **38**, 37 (1974).
5. R. Bonifacio and L. A. Lugiato, Phys. Rev. A **11**, 1507 (1975); Phys. Rev. A **12**, 587 (1975).
6. J. C. MacGillivray and M. S. Feld, Phys. Rev. A **14**, 1169 (1976); Phys. Rev. A **23**, 1334 (1981).
7. N. Scribanovich, I. P. Herman, J. C. MacGillevray, and M. S. Feld, Phys. Rev. Lett. **30**, 309 (1973).
8. H. M. Gibbs, Q. H. F. Vrehen, and H. M. J. Hikspoors, Phys. Rev. Lett. **39**, 547 (1976).
9. A. Flusberg, T. Mossberg, and S. R. Hartman, Phys. Lett. A **58**, 373 (1976).
10. R. Florian, L. O. Schwan, and D. Schmid, Solid State Commun. **42**, 55 (1982); Phys. Rev. A **28**, 2709 (1984).
11. M. S. Malcuit, J. J. Maki, D. J. Simkin, and R. W. Boyd, Phys. Rev. Lett. **59**, 1189 (1987).
12. Yu. V. Nabokin, V. V. Samartsev, and N. B. Silaeva, Izv. Akad. Nauk SSSR, Ser. Fiz. **47**, 74 (1983).
13. P. V. Zinov'ev, S. V. Lopina, Yu. V. Nabokin, N. B. Silaeva, V. V. Samartsev, and Yu. E. Sheibut, Sov. Phys. JETP **58**, 1129 (1983).
14. F. Auzel, S. Hubert, and D. Meichenin, Europhys. Lett. **7**, 459 (1988).
15. C. Greiner, B. Boggs, and T. W. Mossberg, Phys. Rev. Lett. **85**, 3793 (2000).
16. Yu. F. Kiselev, A. F. Prudkoglyad, A. S. Shumovskii, and V. I. Yukalov, Sov. Phys. JETP **67**, 413 (1988).

17. N. A. Bazhanov, D. S. Bulyanitsa, A. I. Zaitsev, A. I. Kovalev, V. A. Malyshev, and E. D. Trifonov, Sov. Phys. JETP **70**, 1128 (1990).
18. V. I. Yukalov, Phys. Rev. Lett. **75**, 3000 (1995).
19. D. S. Druzhin, D. S. Bulyanitsa, and E. D. Trifonov, J. Exp. Theor. Phys. **91**, 239 (2000).
20. V. I. Yukalov and E. P. Yukalova, Phys. Part. Nucl. **35**, 348 (2004).
21. J. Vanacken, S. Stroobants, M. Malfait, et al., Phys. Rev. B **70**, 220401(R) (2004).
22. M. G. Benedict, P. Foeldi, and F. M. Peeters, Phys. Rev. B **72**, 214430 (2005).
23. V. I. Yukalov and E. P. Yukalova, Laser Phys. Lett. **8**, 804 (2011).
24. C. Ohae, A. Fukumi, S. Kuma, et al., J. Phys. Soc. Jpn. **83**, 044301 (2014).
25. T. Brandes, Phys. Rep. **408**, 315 (2005).
26. V. N. Pustovit and T. V. Shahbazyan, Phys. Rev. Lett. **102**, 077401 (2009); Phys. Rev. B **82**, 075429 (2010).
27. V. V. Popov, O. V. Polischuk, A. R. Davoyan, V. Ryzhii, T. Otsuji, and M. S. Shur, Phys. Rev. B **86**, 195437 (2012).
28. R. Fleury and A. Aluù, Phys. Rev. B **87**, 201101(R) (2013).
29. A. Fukumi, S. Kuma, Y. Miyamoto, et al., Prog. Theor. Exp. Phys. 2012, 04D002 (2012).
30. S. Inouye, A. P. Chikkatur, D. M. Stamper-Kurn, J. Stanger, D. E. Pritchard, and W. Ketterle, Science **285**, 571 (1999).
31. M. G. Moore and P. Meystre, Phys. Rev. Lett. **83**, 5202 (1999).
32. E. D. Trifonov, J. Exp. Theor. Phys. **93**, 969 (2001); E. D. Trifonov, Laser Phys. **12**, 211 (2002).
33. Y. A. Avetisyan and E. D. Trifonov, Laser Phys. Lett. **1**, 373 (2004); Laser Phys. Lett. **2**, 512 (2005); Phys. Rev. A **88**, 025601-3 (2013).
34. M. Gross and S. Haroche, Phys. Rep. **93**, 301 (1982).
35. A. V. Andreev, V. I. Emel'yanov, and Yu. A. Il'inskii, Sov. Phys. Usp. **23**, 493 (1980).
36. V. V. Zheleznyakov, V. V. Kocharovskii, and Vl. V. Kocharovskii, Sov. Phys. Usp. **32**, 835 (1989).
37. A. V. Andreev, V. I. Emel'yanov, and Yu. A. Il'inskii, *Cooperative Effects in Optics* (IOP, Bristol, Philadelphia, 1993).
38. M. G. Benedict, A. M. Ermolaev, V. A. Malyshev, I. V. Sokolov, and E. D. Trifonov, *Super-Radiance: Multiatomic Coherent Emission* (IOP, Bristol, Philadelphia, 1996).
39. A. A. Kalachev and V. V. Samartsev, Coherent Phenomena in Optics (Kazan Gos. Univ., Kazan, 2003) [in Russian].
40. V. A. Malyshev, I. V. Ryzhov, E. D. Trifonov, and A. I. Zaitsev, SPIE Proc. **3239**, 129 (1997).
41. V. A. Malyshev, I. V. Ryzhov, E. D. Trifonov, and A. I. Zaitsev, Laser Phys. **8**, 494 (1998).
42. J. T. Manassah and B. Gross, Opt. Commun. **150**, 189 (1998).
43. A. I. Zaitsev, V. A. Malyshev, E. D. Trifonov, and I. V. Ryzhov, J. Exp. Theor. Phys. **88**, 278 (1999); Opt. Spectrosc. **87**, 755 (1999).
44. V. Kozlov, O. Kocharovskaya, Yu. Rostovtsev, and M. Scully, Phys. Rev. A **60**, 1598 (1999).
45. I. V. Ryzhov, N. A. Vasil'ev, I. S. Kosova, M. D. Shtager, and V. A. Malyshev, Opt. Spectrosc. **120**, 440 (2016).
46. V. A. Malyshev, I. V. Ryzhov, E. D. Trifonov, and A. I. Zaitsev, Laser Phys. **9**, 876 (1999).
47. A. I. Zaitsev, I. V. Ryzhov, E. D. Trifonov, and V. A. Malyshev, Opt. Spectrosc. **87**, 956 (1999).
48. A. I. Zaitsev and I. V. Ryzhov, Opt. Spectrosc. **89**, 601 (2000); Opt. Spectrosc. **91**, 941 (2001).
49. A. A. Bogdanov, A. I. Zaitsev, and I. V. Ryzhov, Opt. Spectrosc. **89**, 935 (2000).
50. I. V. Ryzhov, A. I. Zaitsev, and E. V. Shuval-Sergeeva, Opt. Spectrosc. **112**, 604 (2012).
51. O. A. Kocharovskaya and Ya. I. Khanin, JETP Lett. **48**, 630 (1988).
52. Ya. I. Khanin and O. A. Kocharovskaya, J. Opt. Soc. Am. B **7**, 2016 (1990).
53. S. E. Harris, Phys. Rev. Lett. **62**, 1033 (1989).
54. O. Kocharovskaya, Phys. Rep. **219**, 175 (1992).
55. F. T. Arecchi and E. Courtens, Phys. Rev. A **2**, 1730 (1970).
56. A. M. Basharov, G. G. Grigoryan, N. V. Znamenskiy, E. A. Manykin, Yu. V. Orlov, A. Yu. Shashkov, and T. G. Yukina, J. Exp. Theor. Phys. **102**, 206 (2006).
57. F. Haake, H. King, G. Schröder, J. Haus, and R. Glauber, Phys. Rev. A **20**, 2047 (1979); Phys. Rev. Lett. **45**, 558 (1980).
58. N. W. Carlson, D. J. Jackson, A. I. Shawlow, M. Gross, and S. Haroch, Opt. Commun. **32**, 350 (1980).
59. R. F. Malikov and E. D. Trifonov, Opt. Commun. **52**, 74 (1984).
60. S. P. Kuznetsov, *Dynamical Chaos* (Fizmatlit, Moscow, 2001) [in Russian].
61. G. Korn and T. Korn, *Mathematical Handbook for Scientists and Engineers* (Nauka, Moscow, 1974; McGraw-Hill, New York, 1961).
62. F. C. Moon, *Chaotic Vibrations: An Introduction for Applied Scientists and Engineers* (Wiley-VCH, Weinheim, 2004).
63. G. Hacken, *Synergetics* (Springer, Berlin, 1978; Mir, Moscow, 1980).
64. Yu. I. Neimark and P. S. Landa, *Stochastic and Chaotic Vibrations* (Nauka, Moscow, 1987) [in Russian].
65. G. Duffing, *Erzwungene Schwingungen bei Veränderlicher Eigenfrequenz und ihre Technische Bedeutung* (Vieweg, Braunschweig, 1918) [in German].
66. A. P. Kuznetsov and S. P. Kuznetsov, *Nonlinear Oscillations* (Fizmatlit, Moscow, 2005) [in Russian].
67. R. F. Malikov, V. A. Malyshev, and E. D. Trifonov, Opt. Spectrosc. **53**, 387 (1982).
68. A. I. Zaitsev, V. A. Malyshev, and E. D. Trifonov, Opt. Spectrosc. **65**, 599 (1988).
69. L. Allen and J. H. Eberly, *Optical Resonance and Two-Level Atoms* (Dover, New York, 1987; Mir, Moscow, 1978).
70. C. W. Thiel, T. Böttger, and R. L. Cone, J. Lumin. **131**, 353 (2011).

71. T. Zhong, J. M. Kindem, E. Miyazono, and A. Faraon, Nat. Commun. **6**, 8206 (2015).

72. M. Zhong, M. P. Hedges, R. L. Ahlefeldt, J. G. Bartholomew, S. E. Beavan, S. M. Wittig, J. J. Longdell, and M. J. Sellars, Nature **517**, 177 (2015).

73. V. A. Zuikov, A. A. Kalachev, V. V. Samartsev, and A. M. Shegeda, Laser Phys. **9**, 951 (1999); Laser Phys. **10**, 364 (2000).

74. V. A. Zuikov, A. A. Kalachev, V. V. Samartsev, and A. M. Shegeda, Quantum Electron. **30**, 629 (2000).

75. A. A. Kalachev and V. V. Samartsev, Laser Phys. **12**, 1114 (2002); J. Lumin. **98**, 331 (2002).

76. G. G. Grigoryan, Yu. V. Orlov, E. A. Petrenko, A. Yu. Shashkov, and N. V. Znamenskiy, Laser Phys. **15**, 602 (2005).

77. G. G. Grigoryan, Yu. V. Orlov, A. Yu. Shashkov, T. G. Yukina, and N. V. Znamenskiy, Laser Phys. **17**, 511 (2007).

78. A. M. Basharov, G. G. Grigoryan, N. V. Znamenskii, Yu. V. Orlov, A. Yu. Shashkov, and T. G. Yukina, Quantum Electron. **39**, 251 (2009).

79. A. M. Basharov, N. V. Znamenskii, and A. Yu. Shashkov, Opt. Spectrosc. **104**, 241 (2008).

Translated by N. Wadhwa